Hindawi
International Journal of Photoenergy
Volume 2019, Article ID 5737952, 8 pages
https://doi.org/10.1155/2019/5737952

Research Article

Preparation of Nano-Ag-TiO_2 Composites by Co-60 Gamma Irradiation to Enhance the Photocurrent of Dye-Sensitized Solar Cells

Le Thanh Nguyen Huynh,[1,2] **Viet Hai Le**,[3] **Thanh Long Vo**,[1] **Thi Kim Lan Nguyen**,[4] **Quoc Hien Nguyen**,[4] **and Thai Hoang Nguyen**[1,2]

[1]*Department of Physical Chemistry, Faculty of Chemistry, VNUHCM-University of Science, Ho Chi Minh City, Vietnam*
[2]*Applied Physical Chemistry Laboratory, VNUHCM-University of Science, Ho Chi Minh City, Vietnam*
[3]*Faculty of Materials Science and Technology, VNUHCM-University of Science, Ho Chi Minh City, Vietnam*
[4]*Research and Development Center for Radiation Technology, Vietnam Atomic Energy Institute (VAEI), Ho Chi Minh City, Vietnam*

Correspondence should be addressed to Thai Hoang Nguyen; nthoang@hcmus.edu.vn

Received 19 February 2019; Revised 21 April 2019; Accepted 16 May 2019; Published 12 June 2019

Guest Editor: Petru A. Cotfas

Nano-silver-titanium dioxide (Ag-TiO_2) composites were prepared from commercial TiO_2 (P25, Degussa) and silver nitrate ($AgNO_3$) by gamma Co-60 irradiation method with various initial concentrations of $AgNO_3$. The nano-AgTiO_2 composites are utilized as the photoanode for dye-sensitized solar cells (DSCs). Under full sunlight illumination (1000 W/m^2, AM 1.5), the efficiency of DSCs has improved significantly despite the Ag content of below 1%. The DSC—assembled with 0.75 Ag-TiO_2 (0.75% Ag) photoanode—showed that the photocurrent was significantly enhanced from 8.1 mA.cm^{-2} to 9.5 mA.cm^{-2} compared to the DSCs using bared TiO_2 photoanode. The unchanged open-circuit voltage resulted in the overall energy conversion efficiency to be increased by 25% from 3.75% to 4.86%. Electrochemical impedance spectroscopy (EIS) analysis showed that the charge transfer resistance is reduced when increasing Ag content, demonstrating that the charge transfer at TiO_2/dye interface was enhanced in the presence of silver nanoparticles.

1. Introduction

Research and application of new energy resources are essential approaches to reduce dependence on fossil fuels, and solar energy is considered one of the feasible solutions to solve the world's energy crisis. Dye-sensitized solar cells (DSCs) have promised to replace conventional silicon-based solar cells in the context of using clean solar energy due to their low cost, massive production, and facile process. Thus, DSC technology has been an attractive approach for the large-scale solar panel [1–5]. In DSCs, the cell architecture comprises nanostructured TiO_2 photoanode as an electron conductor, a dye Ru-complex as a light absorber, a redox shuttle for dye regeneration, and a counter electrode to collect electrons and reduce positive charges generated through the cell [1]. Commonly, the DSCs showed efficient solar energy-to-electricity conversion of 10% [1, 6].

Many approaches have been studied to alternately improve the conversion efficiency of DSCs, including researching the novel counter electrode, electrolytes, dyes, and semiconductor photoanode materials. Among these, the photoanode plays a decisive part in determining the performance of cells [1, 7–9]. Many semiconductor materials have been studied to be used as photoanode in DSCs such as TiO_2, ZnO, SnO_2, Nb_2O_3, and $SrTiO_3$. In particular, TiO_2 has been universally used due to its chemical stability, excellent charge transport capability, low cost, and easy preparation [2, 10, 11]. In DSCs, TiO_2 plays three roles: (i) providing a substrate for dye adsorption, (ii) accepting electrons from the dye's excited state, and (iii) transporting the electrons from conduction band of TiO_2 to the conducting

substrate then to the external circuit [11, 12]. TiO_2 possesses a wide bandgap energy in both common structures: anatase at 3.2 eV and rutile at 3.0 eV. To improve the solar energy-to-electricity conversion efficiency, the surface of TiO_2 are modified with metallic ions such as Fe^{3+} and Zn^{2+}, alternatively, metallic nanoparticles such as Au, Ag, and Pt [3, 9, 10, 13, 14]. Study incorporation of Ag nanoparticles onto TiO_2 surface showed that the coupling of semiconductor and metal nanoparticles might yield a photoinduced electron transfer across the interface, which in turn may lead to the increased energy conversion efficiency of DSCs [11, 15–17]. Most of the previous reports showed the enhancement of efficiencies (4.86%) due to the plasmonic effect of Ag nanoparticles at high content (>2.5%) [8]. Many methods have been reported to prepare Ag-TiO_2 composite such as microwave-assisted sol–gel techniques [18], a microwave-hydrothermal technique [19], and UV irradiation [20]. Gamma irradiation has been well known as an effective method due to its simple preparation, massive produce, high efficiency, and eco-friendliness [14, 16, 21].

In this work, we prepared nano-Ag-TiO_2 composites at low Ag content (<1%) via Co-60 gamma irradiation. The nano-Ag-TiO_2 composites were used to prepare the photoanodes for DSCs. The role of Ag on the photoperformance of DSCs were investigated by the current-voltage method and the electrochemical impedance spectroscopy.

2. Experimental

2.1. Materials. TiO_2 (P25, Degussa), $AgNO_3$ (99.9%, Sigma-Aldrich), two types of ethyl cellulose (EC) powders (5-15 mPa·s and 30-50 mPa·s, Sigma-Aldrich), ethanol (95%, Sigma-Aldrich), and terpineol (anhydrous 99.9%, Sigma-Aldrich) were commercially available. Fluorine-doped tin oxide (FTO-TEX-8X, 15 Ω/cm^2) conductive glass substrates (Dyesol, Australia), electrolyte solution HPE (Dyesol, Australia), ruthenium complex dye N719 (Dyesol, Australia), and platinum paste PT1 (Dyesol, Australia) were used to fabricate the cathode of the DSCs.

2.2. Preparation of Nano-Ag-TiO_2 Composites. 4.00 g TiO_2 was dispersed in 20 mL solution of ethanol and distilled water (1/1, *v*/*v*) by magnetic stirring for 30 minutes; then, the solution was vibrated by ultrasound for 30 minutes. 10 mM $AgNO_3$ solution was added to the colloidal solution with the various weight ratios of Ag : TiO_2. The mixtures were irradiated via the gamma-radiation from a Co-60 irradiator in the dose range of 10-30 kGy with a dose rate of 1.3 kGy per hour (VINAGAMMA Center, Ho Chi Minh City). Table 1 details the volume of $AgNO_3$ solution, the weight ratios of Ag : TiO_2, and the dose of gamma-radiation. The irradiated colloidal solutions were centrifuged with speed up 10,000 rpm for 30 minutes to collect the powders; then, the final products were dried in air at 60°C overnight.

2.3. Fabrication of DSCs. DSCs (an active area of 0.2 cm^2) were assembled following our process in previous reports with four steps [22–24].

Table 1: Preparation of Ag-TiO_2 samples by gamma irradiation.

Sample	V_{AgNO_3} (mL)	m_{TiO_2} (g)	Ratio of Ag : TiO_2 (% weight)	Dose γ -irradiation (kGy)
0.25 Ag-TiO_2	9.3	4.0	0.25	13.7
0.50 Ag-TiO_2	18.5	4.0	0.50	20.4
0.75 Ag-TiO_2	27.8	4.0	0.75	27.3

2.3.1. Ag-TiO_2 Printing Paste Preparation. The Ag-TiO_2 printing paste is composed of Ag-TiO_2 (20% wt.), ethyl celluloses (10% wt.), and terpinol (70% wt.). 4.50 g EC (5-15 mPa·s) and 3.50 g EC (30-50 mPa·s) was dissolved in absolute ethanol to form 10% EC solution. 0.40 g nano-Ag-TiO_2 composites and 1.40 g terpineol were added to 2.00 g EC solution. The mixture was sonicated in three steps, each for 30 minutes. The final solution was heated in a vacuum oven at 40°C for 10 hours to remove the ethanol and water.

2.3.2. Photoanode Ag-TiO_2 Preparation. The FTO glass, as a current collector, was first cleaned in a detergent solution via ultrasonic for 15 minutes, and then rinsed with distilled water and ethanol. The FTO glass was soaked into a 40 mM $TiCl_4$ solution at 70°C for 30 minutes and re-washed with distilled water and ethanol. The Ag-TiO_2 paste with a thickness of 12-14 μm was coated on FTO substrate by using screen-printed method. After screen-printing, these coated electrodes were heated at 500°C under airflow for 30 minutes to form the Ag-TiO_2 photoanode.

2.3.3. Platinum Cathode Preparation. The FTO glass was treated in 0.1 M HCl in ethanol in an ultrasonic bath for 15 minutes and washed with acetone. The platinum cathode on the FTO substrate (Pt/FTO) was prepared by the screen-printing method using platinum paste PT1. The cathode Pt/FTO was annealed at 450°C for 30 minutes.

2.3.4. DSC Assembly. Both electrodes were arranged into sandwich-type cells by using a ply of melted surlyn at 190°C for 30 seconds. The dye solution (10 mM N719 in DMF) was injected successively into the cells through a hole in the back of platinum cathode, soaking in 4 hours and removing the DMF solvent. The cell was cleaned with acetonitrile for three times before being injected with electrolyte. The hole was then scaled using a quick-drying adhesive. The DSC assembly was performed in a nitrogen-filled glove-box to avoid oxygen and water.

2.4. Structural Characterization. The crystalline structures of nano-Ag-TiO_2 composites were characterized by X-ray diffractometer D8 Advanced (Bruker, Germany) with a copper anode ($\lambda K\alpha = 1.54$ Å). The XRD patterns were acquired in the 2θ range of 20°-80° (0.02° per second). The particle size of nano-Ag-TiO_2 was analyzed by transmission electron microscopy (TEM) images on a TEM 1400 (JEOL, Japan). The UV-vis spectra of nano-Ag-TiO_2 composites were recorded on a UV-vis spectrophotometer (Jasco-V630,

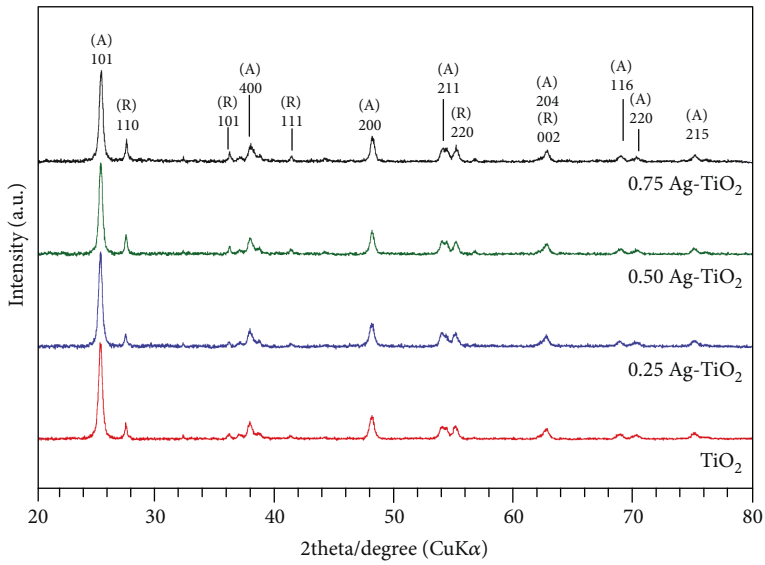

Figure 1: XRD patterns of nano-Ag-TiO_2 composites.

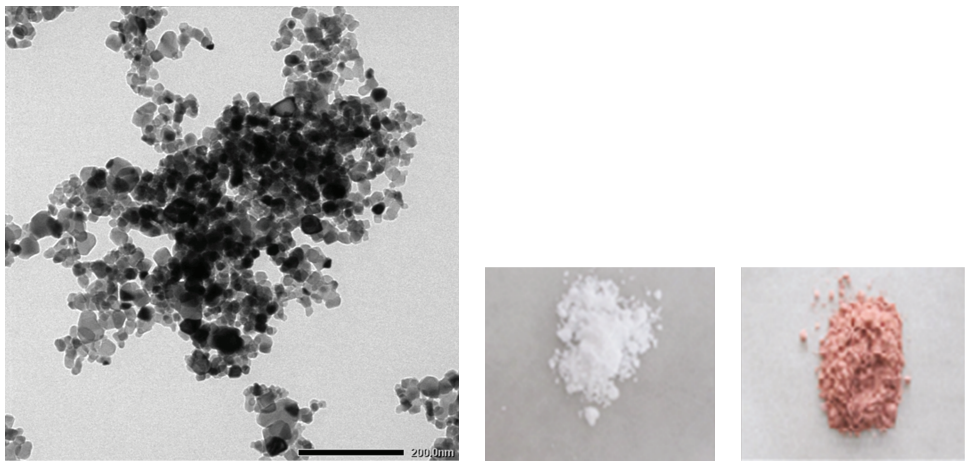

(a) (b) (c)

Figure 2: (a) TEM image of 0.75 Ag-TiO_2 composite. Digital photo of TiO_2 (b) and 0.75 Ag-TiO_2 composite (c).

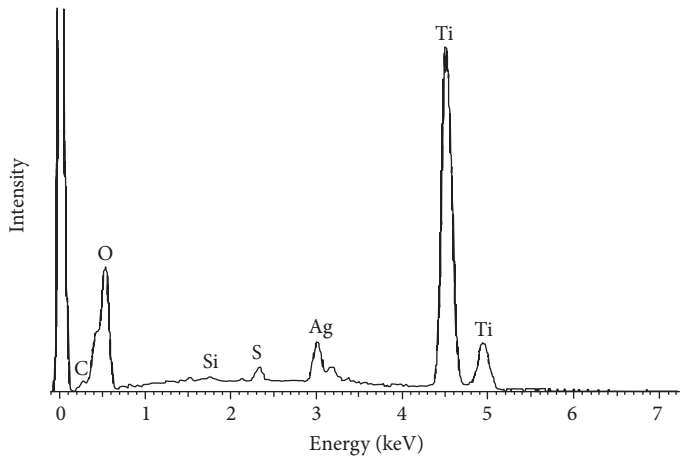

Figure 3: EDS patterns of nano 0.75 Ag-TiO_2 composite.

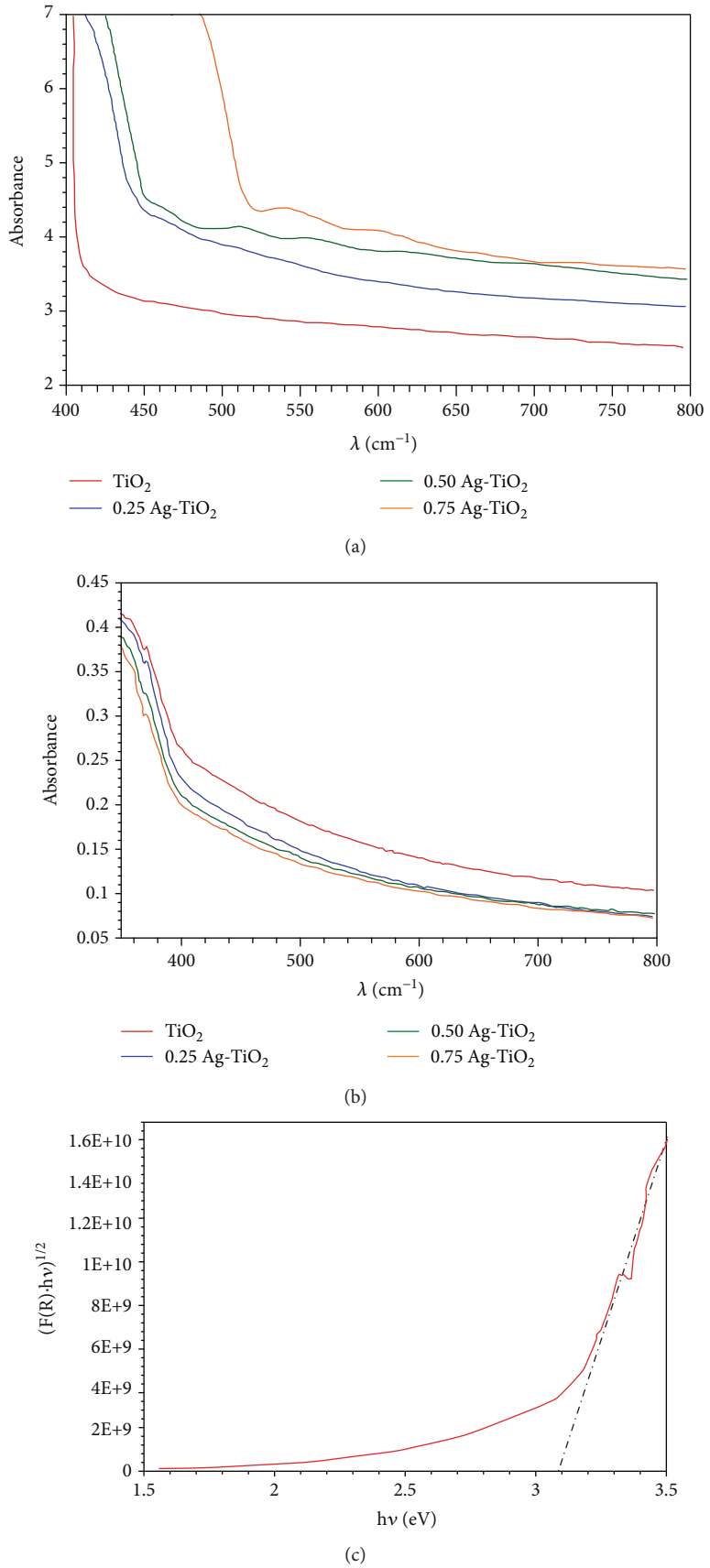

Figure 4: UV-vis absorption spectra of (a) the as-prepared nano-Ag-TiO_2 composites in powder. (b) Ag-TiO_2 photoanode films and (c) Kubelka-Munk plot for TiO_2 photoanode film.

Japan). The chemical composition of the materials was analyzed by EDS method using HITACHI S-4800 FE-SEM/EDS instrument.

2.5. I-V Characterizations. The photovoltaic characteristics (*I-V*) of the cells were recorded by Keithly 2400 source meter. The light source was a solar simulator from a 450 W halogen lamp with an infrared filter (AM 1.5). The incident light intensity was 1000 W/m^2 calibrated with a standard Si solar cell. Electrochemical impedance spectroscopy (EIS) of DSCs was carried out by an AUTOLAB 302N apparatus (Ecochemie, Netherlands) in the frequency range of 0.1 Hz-100 kHz and under illuminations of 1000 W/m^2.

3. Results and Discussion

3.1. Structural Characterization of Nano-Ag-TiO$_2$ Composites. Figure 1 illustrates the XRD patterns of commercial TiO_2 (Degussa P25) and nano-Ag-TiO_2 composites. All diffraction peaks can be indexed in the anatase phase (Tetragonal, space group *I41/amd*) and rutile phase (Tetragonal, space group *P42/mnm*). Structural conservation of TiO_2 indicates that the γ-irradiation with Co-60 irradiator does not affect the crystalline structure of TiO_2 as well as the ratio of anatase phase and rutile phase. No diffraction peak of Ag was observed in XRD patterns of the Ag-TiO_2 samples due to the low content of Ag nanoparticles (below 1%). To determine the existence of Ag naoparticles in composites, other techniques (TEM, EDS, and UV-VIS) were applied.

Figure 2 exhibits the TEM images of the nano 0.75 Ag-TiO_2 composite. We observed the well-defined TiO_2 nanoparticles (bright color) in the range 10-25 nm and the nano-Ag (dark color) on the background of TiO_2 particles. The EDS pattern of 0.75 Ag-TiO_2 (Figure 3) composite powder confirms the existence of Ag on the composite.

Figure 4(a) shows the UV-vis spectra of the samples in powder. We observed that the band-edge absorption of nano-Ag-TiO_2 composites shifted towards the red wavelength (redshift) and the plasmon resonance effect of the silver nanoparticles appeared in the range of wavelength 500-550 nm. The results verified the formation of nano-Ag on TiO_2 by the gamma Co-60 irradiation. Based on the Kubelka-Munk plot, the bandgap energy (E_g) of nano-Ag-TiO_2 composite in powder (Table 2) dropped slightly as compared to TiO_2 ($E_g = 3.1$ eV) following the increase of Ag content.

Following the fabricating process of photoanodes, nano-Ag-TiO_2 composites were calcinated at 500°C for 30 minutes. We keep track of the photoproperties of photoanodes, with the UV-vis spectra visible in Figure 4(b). The UV-vis spectra of photoanodes in Ag-TiO_2 changed significantly. The disappearing of the plasmonic effect in nanosize, as well as the blueshift, was observed due to the agglomeration of Ag nanoparticles after the annealing process. The calculated bandgap of the four photoanodes was approximated in 3.1 eV. Many researches indicated the role of plasmon resonance effect of Ag nanoparticles to increase the performance of DSCs

Table 2: Bandgap energy (E_g) of the as-prepared nano-Ag-TiO_2 composites in powder and Ag-TiO_2 photoanode films, calculated by the Kubelka-Munk plot.

	Bandgap (eV)	
	As-prepared nano-Ag-TiO_2 composites	Ag-TiO_2 photoanode films
TiO_2	3.1	3.1
0.25 Ag-TiO_2	3.1	3.1
0.50 Ag-TiO_2	3.0	3.1
0.75 Ag-TiO_2	2.8	3.1

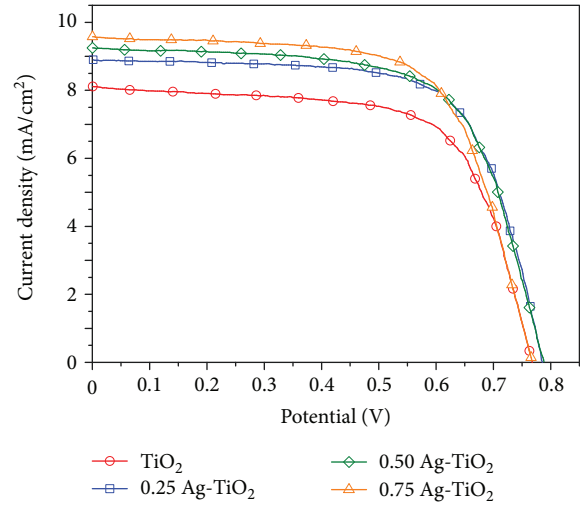

Figure 5: *I-V* curves of DSCs.

Table 3: Performance parameters of DSCs based on photoanodes nano-Ag-TiO_2 and TiO_2-P25.

Sample	V_{oc} (V)	I_{sc} (mA/cm^2)	FF	η (%)
TiO_2	0.77	8.12	0.67	3.75
0.25 Ag-TiO_2	0.79	8.90	0.67	4.83
0.50 Ag-TiO_2	0.79	9.25	0.67	4.88
0.75 Ag-TiO_2	0.77	9.56	0.64	4.86

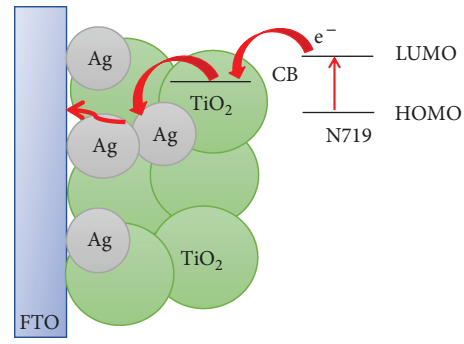

Figure 6: Electron transfer pathway in Ag-TiO_2 photoanode.

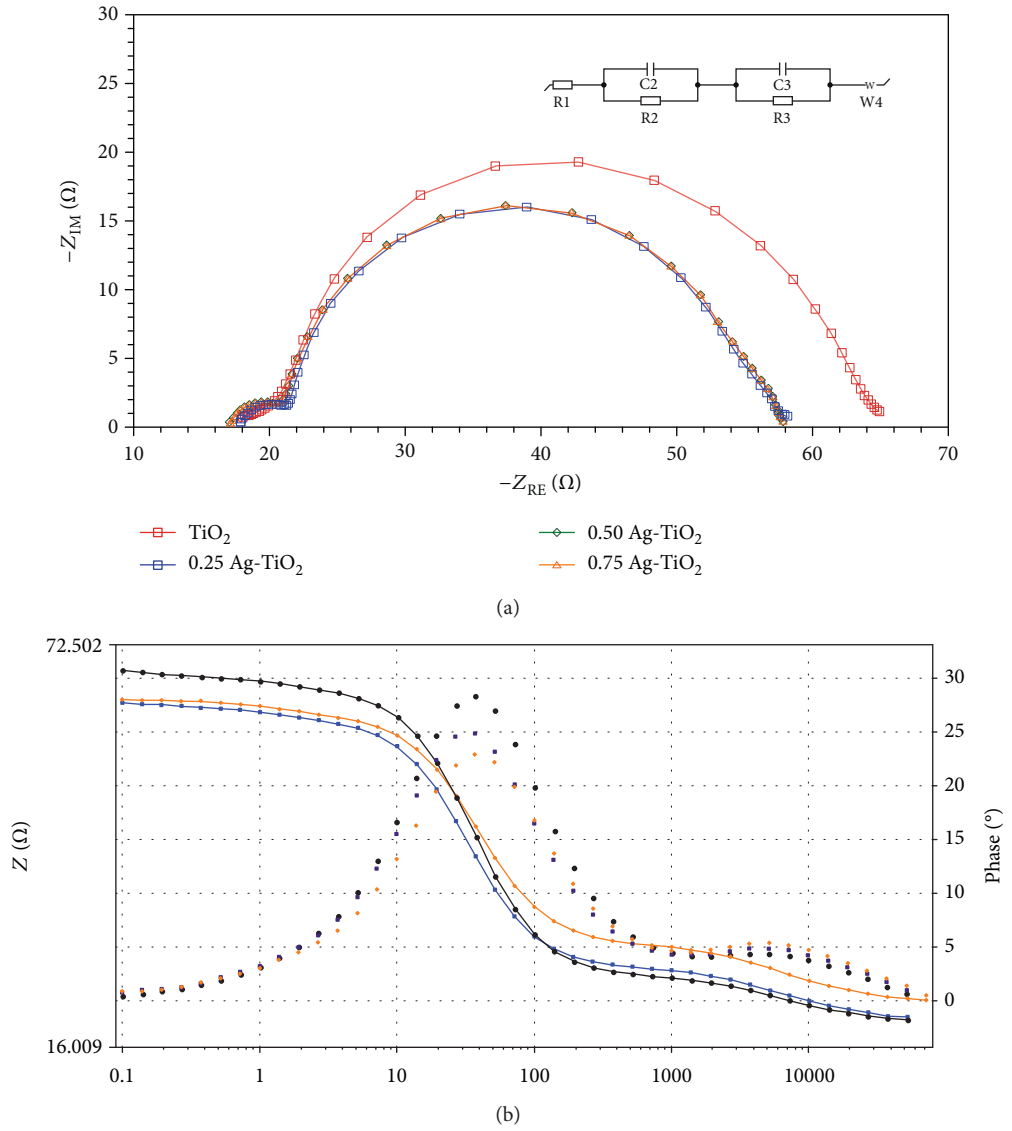

Figure 7: (a) Nyquist plot and (b) Bode-plot of DSCs based on photoanodes nano-Ag-TiO_2 and TiO_2-P25.

Table 4: Cathode charge transfer resistances (R_{ct}) and recombination resistances (R_r) of DSCs measuring at V_{oc} under 1 sun illuminate.

Sample	R_{Pt} (ohms)	R_r (ohms)	C_μ (μF)	τ_n (mS)	f_{max} (Hz)
TiO_2	2.9	43.1	210	7.4	37.3
0.25 Ag-TiO_2	4.1	36.5	233	7.6	37.3
0.50 Ag-TiO_2	4.5	36.6	230	7.2	37.3
0.75 Ag-TiO_2	3.7	36.5	235	6.7	37.3

[11, 16, 19, 25]. The lack of plasmonic effect of low Ag content was detailed in DSCs Performance section.

3.2. DSCs Performances. We fabricated the DSCs using nano-Ag-TiO_2 composites as well as TiO_2-P25 as the photoanode and studied the photoperformance under the 1000 W/m^2 intensity light. The DSCs' performances' results were gathered in Figure 5 and Table 3. The DSCs assembled from TiO_2-P25 photoanode receive a short-circuit current (I_{sc}) of 8.12 mA/cm^2, open-circuit voltage (V_{oc}) of 0.77 V, and fill factor (FF) of 67%; the overall photocurrent conversion efficiency (η) is calculated to be 3.75%. In the case of Ag-TiO_2 photoanodes, the photoperformance of DSCs essentially increased. It is noted that the open-circuit voltages (V_{oc}) were nearly unchanged and stabilized around 0.77 V, indicating that the energy structure of photoanodes (Fermi level) is unvaried. The short-circuit current (I_{sc}) enhanced gradually with the Ag content; particularly, the 0.75 Ag-TiO_2 photoanode exhibited the highest I_{sc} to 9.56 mA/cm^2 as compared to 8.12 mA/cm^2 with TiO2-P25 photoanode. The photoefficiency (η) also improved significantly to 4.86%. We believed that the Ag nanoparticles at low content played as the electron-bridge between TiO_2 and the current collector FTO which limited the grain boundaries' effect across the TiO_2 matrix. We described the mechanism of photoelectron transfer of Ag-TiO_2 photoanodes in DSCs in

Figure 6. When the photoanodes Ag-TiO_2/N719 were illuminated under sunlight AM 1.5, N719 dye was excited and transformed to N719* following by ultra-fast electron injection from N719* to the conduction band (CB) of TiO_2 semiconductor. Due to the lower energy (Fermi level) of Ag-CB than TiO_2-CB, the photoelectrons can collect on Ag particles and transfer facilely in TiO_2 matrix to the current collector FTO. Moreover, the recombination of e_{CB}^- and h^+_{VB} on TiO_2 particles can be restricted which also enhances the photocurrent in DSCs.

To clarify the role of Ag-TiO_2 photoanodes on the photoefficiency of DSCs, the electrochemical impedance spectroscopy (EIS) was performed at the V_{oc} under illuminations of 1000 W/m^2 in the frequency range of 0.1 Hz-100 kHz. The Nyquist plots and Bodes plots are presented in Figure 7; the analysis of EIS spectra is detailed in Table 4. The equivalent circuit is given in the inset of Figure 7. The EIS spectra of DSCs in Nyquist plot (Figure 7(a)) show two semicircles, corresponding to two processes: (i) electron transfer in cathode platinum and (ii) electron transfer in TiO_2 network and from TiO_2-CB to triiodide in electrolyte *via* reaction (1), called recombination-process.

$$TiO_2/e + I_3^- \rightarrow TiO_2 + 3I^- \quad (1)$$

At high frequencies, we observed a negligible variation of electron transfer resistance (R_{Pt}) in cathode platinum. At intermediate frequencies, the recombination resistances (R_r) were decreased drastically (from 43.1 Ω for photoanode TiO_2 and 36.6 Ω for photoanodes Ag-TiO_2) that reveal the role of Ag electron-bridge to facilitate the electron transfer in TiO_2 network. According to the research of Wang et al. [4], the reducing recombination resistance R_r reflects the fast electron transfer in the photoanode whereby the photoperformances were beneficial. Moreover, the chemical capacitance of conduction band electron (C_μ) was also increased that indicated the electron lifetime (τ_n)—composed of resistance and capacitance ($\tau_n = R_r C_\mu$)—was slightly decreased. Furthermore, the characteristic frequency of R_r was stabilized at 37.3 Hz in Bode plots (Figure 7(b)), indicating stable free electron lifetime.

4. Conclusions

In conclusion, we demonstrate the direct preparation of nano-Ag-TiO2 composites by the γ-irradiation method from a Co-60 irradiator and the Ag-TiO_2 showed a capability as photoanode in dye-sensitized solar cells. The DSCs—based on nano-0.75 Ag-TiO_2 composite photoanode—presented an encouraging performance with V_{oc} of 077 V, I_{sc} of 9.56 mA/cm^2, fill factor of 0.64, and photoefficiency of 4.86%. Studying the role of Ag by EIS, we observe only a reduction of recombination resistance in photoanode due to the formation of Ag electron-bridge that improves the electron transfer process but do not reduce electron lifetime.

Data Availability

The data used to support the findings of this study are included within the article.

Conflicts of Interest

The authors declare that there is no conflict of interest regarding the publication of this paper.

Acknowledgments

This research work was supported by Vietnam National University Ho Chi Minh City through grant number HS2015-18-01.

References

[1] B. O'Regan and M. Grätzel, "A low-cost, high-efficiency solar cell based on dye-sensitized colloidal TiO2 films," *Nature*, vol. 353, no. 6346, pp. 737–740, 1991.

[2] T. Ma, M. Akiyama, E. Abe, and I. Imai, "High-efficiency dye-sensitized solar cell based on a nitrogen-doped nanostructured titania electrode," *Nano Letters*, vol. 5, no. 12, pp. 2543–2547, 2005.

[3] X. Lü, X. Mou, J. Wu et al., "Improved-rerformance dye-sensitized solar cells using Nb-doped TiO_2 electrodes: efficient electron injection and transfer," *Advanced Functional Materials*, vol. 20, no. 3, pp. 509–515, 2010.

[4] Y. F. Wang, J. H. Zeng, and Y. Li, "Silver/titania nanocable as fast electron transport channel for dye-sensitized solar cells," *Electrochimica Acta*, vol. 87, pp. 256–260, 2013.

[5] R. Mori, T. Ueta, K. Sakai et al., "Organic solvent based TiO_2 dispersion paste for dye-sensitized solar cells prepared by industrial production level procedure," *Journal of Materials Science*, vol. 46, no. 5, pp. 1341–1350, 2011.

[6] M. Grätzel, "Dye-sensitized solar cells," *Journal of Photochemistry and Photobiology C: Photochemistry Reviews*, vol. 4, no. 2, pp. 145–153, 2003.

[7] Y. Li, M. Ma, W. Chen, L. Li, and M. Zen, "Preparation of Ag-doped TiO_2 nanoparticles by a miniemulsion method and their photoactivity in visible light illuminations," *Materials Chemistry and Physics*, vol. 129, no. 1-2, pp. 501–505, 2011.

[8] S. P. Lim, A. Pandikumar, N. M. Huang, and H. N. Lim, "Enhanced photovoltaic performance of silver@titania plasmonic photoanode in dye-sensitized solar cells," *RSC Advances*, vol. 4, no. 72, pp. 38111–38118, 2014.

[9] S. Ito, T. N. Murakami, P. Comte et al., "Fabrication of thin film dye sensitized solar cells with solar to electric power conversion efficiency over 10%," *Thin Solid Films*, vol. 516, no. 14, pp. 4613–4619, 2008.

[10] Y. Duan, N. Fu, Q. Liu et al., "Sn-doped TiO_2 photoanode for dye-sensitized solar cells," *Journal of Physical Chemistry C*, vol. 116, no. 16, pp. 8888–8893, 2012.

[11] W. Peng, Y. Zeng, H. Gong, Y. Leng, Y. Yan, and W. Hu, "Silver-coated TiO_2 electrodes for high performance dye-sensitized solar cells," *Solid-State Electronics*, vol. 89, pp. 116–119, 2013.

[12] E. Schüler, A.-K. Gustavsson, S. Hertenberger, and K. Sattler, "Solar photocatalytic and electrokinetic studies of TiO_2/Ag

nanoparticle suspensions," *Solar Energy*, vol. 96, pp. 220–226, 2013.

[13] E. Grabowska, A. Zaleska, S. Sorgues et al., "Modification of titanium(IV) dioxide with small silver nanoparticles: application in photocatalysis," *Journal of Physical Chemistry C*, vol. 117, no. 4, pp. 1955–1962, 2013.

[14] T. Harifi and M. Montazer, "Fe^{3+}:Ag/TiO_2 nanocomposite: synthesis, characterization and photocatalytic activity under UV and visible light irradiation," *Applied Catalysis A: General*, vol. 473, pp. 104–115, 2014.

[15] H. Yu, S. Zhang, H. Zhao, B. Xue, P. Liu, and G. Will, "High-performance TiO_2 photoanode with an efficient electron transport network for dye-sensitized solar cells," *Journal of Physical Chemistry C*, vol. 113, no. 36, pp. 16277–16282, 2009.

[16] H. Zhang, G. Wang, D. Chen, X. Lv, and J. Li, "Tuning photoelectrochemical performances of Ag-TiO_2 nanocomposites via reduction/oxidation of Ag," *Chemistry of Materials*, vol. 20, no. 20, pp. 6543–6549, 2008.

[17] P. V. Kamat, "Manipulation of charge transfer across semiconductor interface. A criterion that cannot be ignored in photocatalyst design," *Journal of Physical Chemistry Letters*, vol. 3, no. 5, pp. 663–672, 2012.

[18] W. Tongon, C. Chawengkijwanich, and S. Chiarakorn, "Visible light responsive Ag/TiO_2/MCM-41 nanocomposite films synthesized by a microwave assisted sol–gel technique," *Superlattices and Microstructures*, vol. 69, pp. 108–121, 2014.

[19] Q. Xiang, J. Yu, B. Cheng, and H. C. Ong, "Microwave-hydrothermal preparation and visible-light photoactivity of plasmonic photocatalyst Ag-TiO_2 nanocomposite hollow spheres," *Chemistry - An Asian Journal*, vol. 5, p. 1466, 2010.

[20] F. Hossein-Babaei, M. M. Lajvardi, and F. A. Boroumand, "Large area Ag–TiO_2 UV radiation sensor fabricated on a thermally oxidized titanium chip," *Sensors and Actuators A: Physical*, vol. 173, no. 1, pp. 116–121, 2012.

[21] O. Tahiri Alaoui, A. Herissan, C. Le Quoc et al., "Elaboration, charge-carrier lifetimes and activity of Pd-TiO_2 photocatalysts obtained by gamma radiolysis," *Journal of Photochemistry and Photobiology A: Chemistry*, vol. 242, pp. 34–43, 2012.

[22] T. H. Nguyen, H. M. Tran, and T. P. T. Nguyen, "Application of electrochemical impedance spectroscopy in characterization of mass- and charge transfer processes in dye-sensitized solar cells," *ECS Transactions*, vol. 50, no. 51, pp. 49–58, 2013.

[23] T. H. Thanh, Q. V. Lam, T. H. Nguyen, and T. D. Huynh, "Performance of CdS/CdSe/ZnS quantum dot-sensitized TiO_2 mesopores for solar cells," *Chinese Optics Letters*, vol. 11, no. 7, pp. 072501–072504, 2013.

[24] N. V. Le, H. T. Nguyen, H. V. Le, and T. T. P. Nguyen, "Lead sulfide cathode for quantum dot solar cells: electrosynthesis and characterization," *Journal of Electronic Materials*, vol. 46, no. 1, pp. 274–281, 2017.

[25] S. P. Lim, Y. S. Lim, A. Pandikumar et al., "Gold–silver@TiO_2 nanocomposite-modified plasmonic photoanodes for higher efficiency dye-sensitized solar cells," *Physical Chemistry Chemical Physics*, vol. 19, no. 2, pp. 1395–1407, 2017.